KIDNEY ABNORMALITY DETECTION USING SEGMENTATION-GUIDED CLASSIFICATION ON COMPUTED TOMOGRAPHY IMAGES

JOYITA FARUK[1], SAADIA BINTE ALAM[1], SK SADIA TASNIM ELMA[1], SEFATUL WASI[1], RASHEDUR RAHMAN[2], SYOJI KOBASHI[2]

[1]Department of Computer Science and Engineering, Independent University, Bangladesh, Dhaka 1299, Bangladesh
[2]University of Hyogo, 2167 Shosha, Himeji, Hyogo, Japan
E-MAIL: joyitafaruk@gmail.com, saadiabinte@iub.edu.bd, sksadiatasnim460@gmail.com, sefatulwasi@gmail.com, rashed.rahman@ieee.org, kobashi@eng.u-hyogo.ac.jp

Abstract:

Kidney cancer currently has the 14th highest incidence rate globally. Abnormal growths such as tumors and cysts in the kidney can be malignant and lead to cancer. The current method employed by nephrologists is manually locating the tumors and cysts from CT scans. However, due to the high incidence rate of kidney cancers, this time-consuming approach puts pressure on nephrologists and may lead to misdiagnoses. To improve the diagnostic process, this study proposes an automatic segmentation-guided classification method that can identify and differentiate between normal kidney areas and abnormal kidney areas that contain tumors, cysts, or both. Thereby, the model can detect abnormal kidney regions. In the proposed method, firstly, TotalSegmentator segmentation model's kidney masks are used to crop kidney regions from the abdominal CTs while generating 2D axial images. Then, ResNet101 is used to classify the images into 'normal' and 'abnormal' classes. The proposed method has a high performance in all metrics with a score of 0.9626 and 0.8670 in recall and precision, respectively.

Keywords:

Kidney abnormality detection; Kidney classification; Kidney segmentation; Kidney tumor; Kidney cyst; Deep learning; Computed tomography

1. Introduction

Kidneys are a pair of symmetrical organs found in the back of the abdomen in the human body. They are essential to major functions in the body such as filtering waste products from the blood, regulating electrolyte balance, and maintaining blood pressure. They also produce the hormone EPO that facilitates red blood cell production. Different types of ailments and diseases can affect the kidney, two major ones being tumors and cysts. These abnormalities can be benign or malignant and may lead to cancer. According to 2022 GLOBOCAN estimates of incidence and mortality worldwide for 36 cancers in 185 countries, kidney cancer has the 14th highest incidence rate, with an estimated 434,419 new cases and 155,702 deaths [1]. Not only that, according to the American Cancer Society's research on US cancer statistics, the incidence of kidney cancers has continued to increase per year by 1.5% [2]. Typically, computed tomography (CT), is widely used for detecting kidney diseases [3]. The current process of diagnosing kidney cancer is manual, relying on the radiologists and nephrologist's expertise to locate the tumors or cysts. This is a time-consuming approach, and as such the high incidence rate can put pressure on the medical personnel. Furthermore, the added pressure may also influence diagnosis rates negatively. As such, an automated process would be desirable, to improve the diagnostic process and thereby give patients better treatment.

In the present literature, computer-aided diagnostic (CAD) methods are the popular approach to automate diagnoses. Specifically, CAD methods employing deep learning, a subset of machine learning that utilizes deep neural networks, have shown promise. Before the advent of deep learning, several studies have achieved automation through traditional machine learning techniques. Jagga used supervised learning algorithms, J48, Random Forest, SMO, and Naïve Bayes, to classify the stages of renal cell carcinoma (RCC) based on gene expression profiles [4]. The highest scores achieved were 89%, 77%, and 0.8 for sensitivity, accuracy, and an area under receiver operating characteristic (ROC) curve, respectively. Anter and Hassenian used a segmentation approach based on a watershed algorithm, neutrosophic sets (NS), and a fast fuzzy c-mean clustering algorithm (FFCM) for CT liver tumor segmentation, achieving an overall accuracy of 0.9498 and a dice score of 0.9288 [5].

However, traditional machine learning falls behind the advantages deep learning can provide today. With traditional means, there is a reliance on feature engineering and it has limited scalability in regards to growing with data. Deep learning employs deep layers to capture complex features and

automatically learns hierarchical features from raw data, so there is no need for manual feature extraction. As medical images feature complex information, deep learning is the leading choice for automatic CAD methods using medical imaging [6]. In particular, convolutional neural networks (CNN) are used in the majority of medical image diagnostic methods [7]. CNNs are exceptionally capable of handling image and video data. As such, various studies are developing CAD methods tackling many problems such as the work on skin lesion diagnosis by Lopez-Labraca et al. [8], and the study by Qian et al. on pituitary tumor detection using MRIs [9].

In the current research sphere, it is evident that there is a large interest in addressing problems regarding kidney tumors. Alzu'bi et. al conducted a study using 2D CNNs for a novel dataset from the King Abdullah University Hospital (KAUH) [10]. A six-layer 2D CNN (CNN-6), a ResNet50 with 50 layers, and a VGG16 with 16 layers were used as kidney segmentation models, and a four-layer 2D CNN (CNN-4) was used for classification. CNN-6 achieved the highest accuracy of 97%. ResNet50, VGG16, and CNN-4 achieved accuracies of 96%, 60%, and 91%, respectively. Bolocan et al. conducted a study for the segmentation and classification of RCC, to distinguish malignant and benign tissues and identify the likely subtype [11]. The dataset consists of four-phase contrast-enhanced CT - pre-contrast, arterial, venous, and excretory phases. They used the European Deep-Health toolkit's Convolutional Neural Network. The mean Dice score for kidney segmentation was 0.84, and tumor segmentation was 0.675, while the RCC classification accuracy was 0.885.

To further facilitate solutions, the KiTS19 Kidney Tumor Segmentation Challenge was introduced, inviting researchers to compete on a global scale. It featured a dataset called the KiTS19 and was the first in a challenge series [12]. Subsequent challenge in the series with the respective dataset is KiTS21 [13]. Li et al. used a radiomics-based approach, to automatically classify kidney tumors and normal kidney tissues on the KiTS19 dataset [14]. In total, 837 radiomics features were extracted and 217 were identified after univariate screening. From these, 3 features were selected to establish the binary logistic regression model. The area under the receiver operating characteristic (AUROC) curve for the train set and test set were 0.9798 and 0.9841, respectively. A multi-scale supervised 3D U-Net called the MSS U-Net was developed by Zhao et al. utilizing the KiTS19 dataset [15]. They combined deep supervision with exponential logarithmic loss to increase the 3D U-Net training efficiency, achieving a Dice coefficient of 0.969 for the kidney and 0.805 for the tumor. Rao et al. proposed a weight pruning (WP)-UNet model, which utilized the KiTS19 dataset [16]. It was designed to be a lightweight deep learning model, that involves few parameters, a quick assumption time, and a low floating-point computational complexity. For the kidney tumor region, they obtained a dice score of 0.9799 for the training set and 0.9599 for the validation set.

In this paper, we propose a 2-step segmentation-guided classification approach to detect the abnormal kidney regions affected by tumors, cysts, or both. In the first step, the kidney region is segmented from abdominal CT followed by classifying the kidney regions into normal or abnormal cases. By segmenting the kidney region, the background area is reduced and the classification model focuses on the kidney region only. TotalSegmentator model [17] is used for segmenting the kidney regions and the ResNet101 CNN is used for the classification [18]. The result is compared with prior work that performed classification on the whole CT images using VGG16 by Wasi et. al [19], [20]. Wasi et. al used an active contour algorithm to reduce the background, achieving a recall and precision of 0.9302 and 0.8045, respectively. To determine the efficacy of the segmentation of kidney regions prior to classification, we coupled the kidney region segmentation by TS with VGG16, achieving a recall and precision of 0.9317 and 0.8502. The proposed method with ResNet101 achieved recall and precision of 0.9626 and 0.8670, respectively.

2. Dataset Description

For the objectives of this study, the KiTS21 dataset from the 2021 Kidney Tumor Segmentation Challenge is used [13]. The dataset contains CT images from 300 patients who went through partial or radical nephrectomy for suspected malignancy in the renal area. The dataset was collected from M Health Fairview and Cleveland Clinic Medical Center. There was a challenge preceding the 2021 challenge, the 2019 Grand Challenge, which included the same 300 cases. However, the 2021 version has added 'cyst' as a semantic class, resulting in 3 total classes of 'cyst',' tumor', and 'kidney'.

The CT images are in the format of 'imaging' NIFTI (Neuroimaging Informatics Technology Initiative) extension files. They have three channels, corresponding to the axial, coronal, and sagittal planes. The coronal and sagittal planes consist of 512-pixel channels, while the axial plane is variable, ranging from 29 to 1059. The thickness of the slices varies from 0.5-5mm and the resolution varies from 0.437-1.041mm per pixel.

Alongside the CT images, each case also contains three aggregated segmented masks, derived using AND, OR, and major set operations. It is in these masks that the semantic classes have been segmented. For this study's use, the 'aggregated_OR_seg' is used. 0, 1, 2, and 3 correspond to the background, the normal kidney area, the tumor area, and the cyst area respectively.

3. Method

This study proposes a 2-step segmentation-guided approach to detect abnormal kidney areas through the classification of normal kidney areas and abnormal kidney areas that are tumorous or cystic. Figure 1 visualizes the process using a block diagram. The first step is the axial image slice extraction and the segmentation-guided cropping technique using TotalSegmentator kidney masks. The second step is the classification using ResNet101 as the chosen architecture.

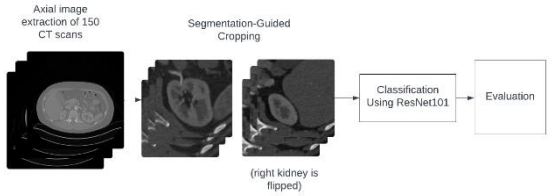

FIGURE 1. Block Diagram of Classification Process

3.1. Preprocessing

To prepare the dataset for classification, a dataset is created from 150 randomly selected cases from the KiTS21 dataset. 2D Portable Network Graphics (PNG) image slices in the axial plane are generated from the 3D CT images. The kidney areas are cropped using segmentation-guided cropping. For this purpose, the TotalSegmentator (TS) segmentation model is selected. Utilizing TS's 'kidney_left' and 'kidney_right' kidney masks, the individual kidney areas are cropped from the 2D PNG images to remove the background as much as possible. To increase the pool of data and better guide the focus of the model's training, the right kidney images are flipped. This is possible as kidneys are almost symmetrical organs. All images are resized to 224x224. Then using the information from the 'aggregated_OR_seg' mask, the images are separated into two overarching classes: 'normal' and 'abnormal'. If pixel values 2 or 3 is found in the mask, then the image is considered an 'abnormal' class as 2 represents tumor and 3 represents cyst area. Other images are classified as 'normal'. The train, test, and validation split are 80%, 10%, and 10% respectively, with the corresponding image counts being 15970, 1995, and 1995. In train set, the abnormal image count is 4741 and, in test, and validation sets, the abnormal image counts are 592 each. The standard deviation of images per case is 133.67, with range from 25 to 508.

3.2. TotalSegmentator

A state-of-the-art segmentation model TotalSegmentator (TS) is employed for the segmentation-guided cropping [17]. Based on the nnU-Net architecture, it is a self-adapting model capable of segmenting 104 anatomical structures. Although TS is capable of rendering segmentations of 3mm resolution, to enhance speed and keep computational costs low, the 'fast' method is used, which renders 1.5mm resolution kidney masks. The 'kidney_left' and the 'kidney_right' masks are used to calculate the bounding boxes of the individual kidney regions. The bounding boxes are then used to crop the generated axial slices to each kidney region. For each kidney of each case, a 3D bounding box is calculated from the TotalSegmentator kidney masks by finding the maximum and minimum coordinates of the kidney area in the 3 planes, x, y, and z. Then, to avoid the error of kidney edges being cut off, a 20% expansion is applied to these coordinates to achieve the cropped region coordinates. Using these coordinates, the slices are cropped, resulting in two images of each kidney. This process is depicted in Fig. 2.

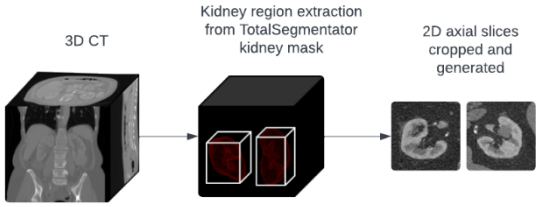

FIGURE 2. Segmentation-guided Cropping Process

3.3. ResNet101

In this paper, the ResNet101 model from the TensorFlow Keras applications library is utilized for the classification. ResNet is a deep learning CNN architecture developed by Kaiming He et. al [18]. Two main components of ResNet are the residual block, that learns the difference between the input and the output, and the skip connections, that reduce the vanishing gradient problem. ResNet101 contains 101 layers. The residual blocks follow a bottleneck design, which consists of three convolutional layers with kernel size of: 1×1, 3×3, and 1×1.

3.4. VGG16

The VGG16 model from the TensorFlow Keras applications library is utilized for comparison to the prior work with VGG16 [20]. The VGG16 is a CNN architecture designed by Simonyan and Zisserman with the goal of increasing depth by using small convolutional filters [19]. VGG16 is a version of the base VGG architecture with 16 weighted layers. The convolutional layers in VGG16 use 3×3 filters with a stride of 1.

3.5. Fine-tuning

The transfer learning technique is used for training [21]. Using this technique, a CNN model trained for one task can be used as the base to train for a new task. The CNN model is pre-trained on a large dataset, in this case, ImageNet for classification. Then the pre-trained CNN model is trained on the target dataset. This step is referred as 'fine-tuning'. When fine-tuned with a new dataset, the model is capable of expanding on the previous knowledge base and learning the relevant features from the new dataset. It allows for reduced training time and is advantageous in cases where the dataset is sufficiently large to train a deep CNN. For our objective, the layers added on top of the pre-trained ResNet101 and VGG16 models are as follows: two dense layers with 1024 units and rectified linear unit (ReLu) activation, one flatten layer, and one dense layer with 2 units according to the number of classes.

4. Evaluation

The evaluation metrics used are precision, recall, and the area under the receiver operating characteristic (AUROC) curve. To calculate precision and recall, the number of true positives (TP), true negatives (TN), false positives (FP), and false negatives (FN) are calculated. TP and TN are the number of correctly predicted images, while FP and FN are the number of incorrectly predicted images. To visualize these metrics, a confusion matrix is used. A confusion matrix is a tool used when calculating and visualizing a classification model. It is a table where the primary diagonal shows the TP and TN, while the secondary diagonal shows the FP and FN. The precision is the accuracy of the positive predictions. Recall is the rate of the correctly predicted positive instances among all the ground truth positives. They are calculated using the following equations:

$$Precision = \frac{TP}{(TP+FP)} \quad (1)$$

$$Recall = \frac{TP}{(TP+FN)} \quad (2)$$

5. Results and Discussion

The proposed method with ResNet101 with prior TS segmentation performed highly, achieving a score of 86.70% and 96.26% in precision and recall respectively, as shown in Table 1. The high recall score displays the model's competent performance in accurately detecting the abnormal regions by differentiating them from the normal regions. The precision displays that it has a high rate of correctly identified positive predictions. The confusion matrix in Table 2 visualizes the TP, TN, FP, and FN values for ResNet101. A total of 515 abnormal TP predictions were made. The AUROC for ResNet101 is 0.986 and 0.984 for abnormal and normal respectively, shown in Fig. 3. The curve shows that the false positive rate for the model is very low and the true positive rate is very high, close to the ideal AUROC score of 1. The minuscule difference in the scores for abnormal and normal also shows the model's consistency in performance when classifying both classes.

TABLE 1. Average Recall and Precision for ResNet101

Metric	Score
Recall	0.9626
Precision	0.8670

TABLE 2. Confusion Matrix of ResNet101

Actual Labels	Predicted Labels	
	Abnormal	*Normal*
Abnormal	515	79
Normal	20	1381

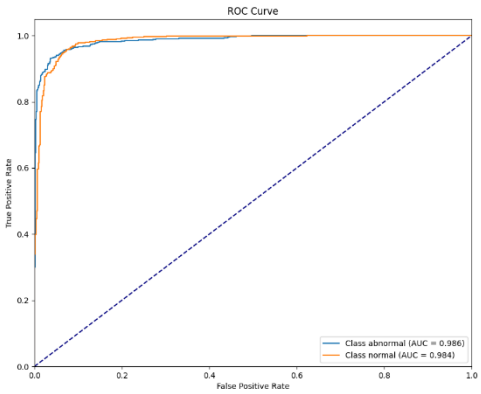

FIGURE 3. ResNet101 AUROC Curve

To see the effectiveness of the segmentation of kidney regions prior to classification, we combined the kidney region segmentation by TS with VGG16 and compared it to the prior work done by Wasi et. al with VGG16 [20]. Table 3 shows that VGG16 with prior segmentation has achieved a precision and recall score of 85.02% and 93.17% respectively. A total of 505 abnormal TP predictions were made as shown in Table 4. The proposed method combined with VGG16 outperformed

VGG16 [20] in both recall and precision, as shown in Table 5. Wasi et. al used the same KiTS21 dataset, and trained on axial images as well. However, they used an active contour algorithm in their preprocessing to subtract the background while generating 2D axial images, with a focus on the abdominal area. Conversely, in the proposed method, firstly the kidneys were segmented and then the images were cropped with a calculated bounding box that focused on the kidney region only. This improved the model's learning as the differences between the classes are better highlighted in a more concentrated focal point. In the broader perspective, the improvement also shows that preprocessing has a significant role in achieving better classification results. The proposed method combined with VGG16 has improved the precision by 0.0457. This suggests that the segmentation-guided cropping method is more successful at reducing the false negatives and better at identifying the positive ground truths. ResNet101 achieved even better results, outperforming both VGG16 models as shown in Table 5. In contrast to VGG16 model's 16 layers, ResNet101 has 101 layers. This deeper learning is possible due to the skip connections of ResNet101 model which mitigates the vanishing gradient problem. Thus, the proposed method with ResNet101 was more successful at learning the complex features of the abnormal and normal kidney regions.

TABLE 3. Average Recall and Precision for VGG16 with prior kidney segmentation by TS

Metric	Score
Recall	0.9317
Precision	0.8502

TABLE 4. Confusion Matrix of VGG16 with prior kidney segmentation by TS

Actual Labels	Predicted Labels	
	Abnormal	*Normal*
Abnormal	505	89
Normal	37	1364

TABLE 5. Comparison of the proposed method and prior work

Metric	Architecture		
	Proposed method using TS & ResNet101	*VGG16 with prior TS segmentation*	*VGG16 [20]*
Recall	0.9626	0.9317	0.9302
Precision	0.8670	0.8502	0.8045

6. Conclusion

This study aims to develop an automated process for the classification of normal kidney areas and abnormal kidney areas that are tumorous or cystic. To achieve this, a 2-step segmentation-guided classification method is proposed. Firstly, the kidney masks are generated by TS, using which bounding boxes are calculated to crop to the kidney area while generating 2D axial images. Secondly, ResNet101 CNN is trained on the cropped images for classification. The results showcase competent performance, with the proposed method achieving 0.9317, 0.8502, 0.986, and 0.984 at recall, precision, abnormal AUROC, and normal AUROC respectively. A comparison was conducted with a different VGG16 classification model that used the KiTS21 dataset and active contour algorithm for preprocessing. The proposed method achieved 3.34% and 6.25% better scores in recall and precision respectively, displaying the advantage of the segmentation-guided cropping. However, there are three limitations we aim to address in the future. Firstly, as this is a preliminary study, out of 300 cases of the KiTS21 dataset, 150 were used. The results may be further improved upon including the rest of the cases. In the future, our work will be expanded to include all the cases. Secondly, only ResNet101 and VGG16 have been used to test the proposed method. Further exploration of models and comparison is necessary to find an optimal model. Thirdly, we have not attempted further explainability such as visualization techniques like Grad-CAM. Additionally, while classification is one step of the diagnostic process, there are further succeeding steps necessary for automation. The next problem to address should be the localization of the abnormal region. Another important aspect of future work should be the incorporation of coronal and sagittal plane images in training.

References

[1] Freddie. Bray, Mathieu. Laversanne, Hyuna. Sung, Jacques. Ferlay, Rebecca. Siegel, Isabelle. Soerjomataram, and Ahmedin. Jemal, "Global cancer statistics 2022: GLOBOCAN estimates of incidence and

mortality worldwide for 36 cancers in 185 countries", CA: A Cancer Journal for Clinicians, Vol. 74, No. 3, pp. 229-263, April 2024.

[2] Rebecca. L. Siegel, Angela. N. Giaquinto, and Ahmedin. Jemal, "Cancer statistics, 2024", CA: A Cancer Journal for Clinicians, Vol. 74, No. 1, pp. 12-49, January 2024.

[3] W. Bai, Y. Fadil, A. Chadli, M. Dakir, A. Debbagh, and R. Aboutaeib, "Correlation between CT and anatomopathological staging of kidney cancer", International Journal of Surgery Case Reports, Vol. 80, Art. No. 105687, March 2021.

[4] Zeenia. Jagga, "Classification models for clear cell renal carcinoma stage progression, based on tumor RNAseq expression trained supervised machine learning algorithms", Proceeding of BMC Proceedings 8, Cincinnati, May 2014.

[5] Ahmed. M. Anter, and Aboul. E. Hassenian, "CT liver tumor segmentation hybrid approach using neutrosophic sets, fast fuzzy c-means and adaptive watershed algorithm", Artificial Intelligence in Medicine, Vol. 97, pp. 105-117, June 2019.

[6] Zakaria. Rguibi, Hajami. Abdelmajid, and Dya. Zitouni, "Deep Learning In Medical Imaging: A Review", in Applications of Machine intelligence in Engineering, 1st ed., J. K. Mandal, S. Misra, J. S. Banerjee and S. Nayak, Eds. Boca Raton (Florida), USA: CRC Press, 2022., Ch. 15.

[7] Ahmad. W. Salehi, Shakir. Khan, Gaurav. Gupta, Bayan. I. Alabduallah, Abrar. Almjally, Hadeel. Alsolai, Tamanna. Siddiqui, and Adel. Mellit, "A Study of CNN and Transfer Learning in Medical Imaging: Advantages, Challenges, Future Scope", Sustainability, Vol. 15, No. 7, Art. No. 5930, March 2023.

[8] Javier. López-Labraca, Iván. González-Díaz, Fernando. Díaz-de-María, and Alejandro. Fueyo-Casado, "An interpretable CNN-based CAD system for skin lesion diagnosis", Artificial Intelligence in Medicine, Vol. 132, August 2022.

[9] Yu. Qian, Yue. Qiu, Cheng-Cheng. Li, Zhong-Yuan. Wang, Bo-Wen. Cao, Hong-Xin. Huang, Yi-Hong. Ni, Lu-Lu. Chen, and Jin-Yu Sun, Pituitary, Vol. 3, No. 1, June 2020.

[10] Dalia. Alzu'bi, Malak. Abdullah, Ismail. Hmeidi, Rami. AlAzab, Maha. Gharaibeh, Mwafaq. El-Heis, Khaled. H. Almotairi, Agostino. Forestiero, Ahmad. M. Hussein, and Laith. Abualigah, "Kidney Tumor Detection and Classification Based on Deep Learning Approaches: A New Dataset in CT Scans", Journal of Healthcare Engineering, Vol. 2022, No. 1, pp. 1-22, October 2022.

[11] Vlad-Octavian. Bolocan, Mihaela. Secareanu, Elena. Sava, Cosmin. Medar, Loredana. S. C. Manolescu, Alexandru-Stefan. C. Rasuc, Maria. G. Costache, George. D. Radavoi, Robert-Andrei. Dobran, and Viorel. Jinga, "Convolutional Neural Network Model for Segmentation and Classification of Clear Cell Renal Cell Carcinoma Based on Multiphase CT Images", Journal of Imaging, Vol. 9, No. 12, Art. No. 280, December 2023.

[12] Nicholas. Heller et al., "The KiTS19 Challenge Data: 300 Kidney Tumor Cases with Clinical Context, CT Semantic Segmentations, and Surgical Outcomes," arXiv:1904.00445, 2020.

[13] Nicholas. Heller et al., "The KiTS21 Challenge: Automatic segmentation of kidneys, renal tumors, and renal cysts in corticomedullary-phase CT", arXiv:2307.01984, July 2023.

[14] Yunfei. Li, Xinrui. Gao, Xuemei. Tang, Sheng. Lin, and Haowen. Pang, "Research on automatic classification technology of kidney tumor and normal kidney tissue based on computed tomography radiomics", Frontiers in Oncology, Vol. 13, February 2023.

[15] Wenshuai. Zhao, Dihong. Jiang, Jorge. P. Queralta, and Tomi. Westerlund, "MSS U-Net: 3D segmentation of kidneys and tumors from CT images with a multi-scale supervised U-Net", Informatics in Medicine Unlocked, Vol. 19, June 2020.

[16] Patike. K. Rao, Subarna. Chatterjee, and Sreedhar. Sharma, "Weight Pruning-UNet: Weight Pruning UNet with Depth-wise Separable Convolutions for Semantic Segmentation of Kidney Tumors", Journal of Medical Signals and Sensors, Vol. 12, No. 2, pp. 108-113, May 2022.

[17] Jakob. Wasserthal et. al, "TotalSegmentator: robust segmentation of 104 anatomical structures in CT images", arXiv:2208.05868, July 2023.

[18] Kaiming. He, Xiangyu. Zhang, Shaoqing. Ren, and Jian. Sun, "Deep Residual Learning for Image Recognition", Proceeding of 2016 IEEE Conference on Computer Vision and Pattern Recognition (CVPR), Las Vegas, June 2016.

[19] Karen. Simonyan and Andrew. Zisserman, "Very Deep Convolutional Networks for Large-Scale Image Recognition", Proceeding of International Conference on Learning Representations, Banff, September 2014.

[20] Sefatul. Wasi, Saadia. B. Alam, Rashedur. Rahman, M. A. Amin, and Syoji. Kobashi, "Kidney Tumor Recognition from Abdominal CT Images using Transfer Learning", Proceeding of 2023 IEEE 53rd International Symposium on Multiple-Valued Logic, Matsue, May 2023.

[21] Sinno. J. Pan and Qiang. Yang, "A Survey on Transfer Learning," IEEE Transactions on Knowledge and Data Engineering, Vol. 22, No. 10, pp. 1345-1359, October 2010.